The Plant Cell, Vol. 30: 2512–2528, October 2018, www.plantcell.org © 2018 ASPB.



# Blue Light Regulates Secondary Cell Wall Thickening via MYC2/MYC4 Activation of the *NST1*-Directed Transcriptional Network in Arabidopsis[OPEN]

**Qian Zhang,[a,b] Zhi Xie,[a,b] Rui Zhang,[a,b] Peng Xu,[a,1] Hongtao Liu,[a] Hongquan Yang,[c] Monika S. Doblin,[d] Antony Bacic,[d] and Laigeng Li[a,2]**

[a]National Key Laboratory of Plant Molecular Genetics, CAS Center for Excellence in Molecular Plant Sciences, Shanghai Institute of Plant Physiology and Ecology, Chinese Academy of Sciences, Shanghai 200032, China
[b]University of the Chinese Academy of Sciences, Beijing 100049, China
[c]College of Life and Environmental Sciences, Shanghai Normal University, Shanghai 200234, China
[d]ARC Centre of Excellence in Plant Cell Walls and La Trobe Institute for Agriculture and Food, School of Life Sciences, Department of Animal, Plant, and Soil Sciences, AgriBio, La Trobe University, Bundoora VIC 3086, Australia

ORCID IDs: 0000-0002-7086-6606 (Q.Z.); 0000-0002-7996-3461 (Z.X.); 0000-0001-5864-8713 (R.Z.); 0000-0001-8007-9879 (P.X.); 0000-0002-6363-7450 (H.L.); 0000-0001-6215-2665 (H.Y.); 0000-0002-8921-2725 (M.S.D.); 0000-0001-7483-8605 (A.B.); 0000-0001-6924-4431 (L.L.)

**Secondary cell walls (SCWs) are formed in some specific types of plant cells, providing plants with mechanical strength. During plant growth and development, formation of secondary cell walls is regulated by various developmental and environmental signals. The underlying molecular mechanisms are poorly understood. In this study, we analyzed the blue light receptor *cryptochrome1* (*cry1*) mutant of *Arabidopsis thaliana* for its SCW phenotypes. During inflorescence stem growth, SCW thickening in the vasculature was significantly affected by blue light. *cry1* plants displayed a decline of SCW thickening in fiber cells, while *CRY1* overexpression led to enhanced SCW formation. Transcriptome analysis indicated that the reduced SCW thickening was associated with repression of the *NST1*-directed transcription regulatory networks. Further analyses revealed that the expression of *MYC2*/*MYC4* that is induced by blue light activates the transcriptional network underlying SCW thickening. The activation is caused by direct binding of MYC2/MYC4 to the *NST1* promoter. This study demonstrates that SCW thickening in fiber cells is regulated by a blue light signal that is mediated through MYC2/MYC4 activation of *NST1*-directed SCW formation in Arabidopsis.**

## INTRODUCTION

All plant cells are encased in a wall whose synthesis, deposition, and remodeling is tightly regulated during plant development and in response to biotic and abiotic stresses. When cells are expanding, they deposit a highly hydrated wall, the primary cell wall, that is sufficiently flexible to yield to turgor and of sufficient tensile strength to prevent bursting. Once expansion has ceased, some cells undergo secondary development, such as those of the vasculature (fiber and vessel cells), and deposit "linear" polysaccharides (cellulose and noncellulosic polysaccharides) to form a dehydrated/hydrophobic cell wall, the secondary cell wall (SCW), that is able to withstand enormous compressive forces. SCWs not only provide plants with mechanical support (Hoson and Wakabayashi, 2015) but act as both a defense barrier (Underwood, 2012) and a conduit for long-distance transportation of water and nutrients.

[1]Current address: Department of Genetics and Informatics Institute, University of Alabama, Birmingham, AL 35294.
[2]Address correspondence to lgli@sibs.ac.cn.
The author responsible for distribution of materials integral to the findings presented in this article in accordance with the policy described in the Instructions for Authors (www.plantcell.org) is: Laigeng Li (lgli@sibs.ac.cn).
[OPEN]Articles can be viewed without a subscription.
www.plantcell.org/cgi/doi/10.1105/tpc.18.00315

Lignified SCWs are composed of approximately equal portions of lignin, cellulose, and noncellulosic polysaccharides, and their formation is tightly regulated by a transcriptional regulatory hierarchy to ensure precise spatio-temporal deposition of SCW components in specialized cells (Taylor-Teeples et al., 2015). In *Arabidopsis thaliana*, *VND6* and *VND7* are expressed specifically in xylem, regulating SCW formation in xylem vessels (Yamaguchi et al., 2010), while *NST1* and *SND1* are expressed in fiber cells, regulating SCW formation in interfascicular fibers and xylem fibers (Mitsuda et al., 2005; Zhong et al., 2006), indicating that SCW deposition is controlled in a cell-type-specific manner. NST1, SND1, VND6, and VND7 can bind directly to the promoters of other transcription factor (TF) or cell wall biosynthesis genes to orchestrate a downstream transcriptional regulatory network that controls lignin, cellulose, and noncellulosic polysaccharide biosynthesis in wall-thickened cells (Zhong et al., 2008, 2010; Yamaguchi et al., 2010, 2011; Zhong and Ye, 2014, 2015; Taylor-Teeples et al., 2015).

SCW formation is also regulated by many environmental factors, including light, drought, heat, and pathogens (Le Gall et al., 2015). For example, plants grown in shade conditions have increased cell elongation and decreased cell wall thickening (Sasidharan et al., 2010; Keuskamp et al., 2011; Huber et al., 2014; Wu et al., 2017), whereas plants exposed to UV light have smaller leaves and epidermal cells with thicker walls and cuticles

## IN A NUTSHELL

**Background:** Plant vascular tissues provide plants with mechanical strength and long-distance transportation, and the thickened secondary cell walls of certain types of vascular cells help plants grow upright. Formation of the secondary cell wall is regulated by environmental and developmental signals. However, little is known about how light, temperature, and other environmental signals regulate secondary cell wall formation.

**Question:** We were interested in determining whether light contributes to regulating secondary cell wall thickening and, if so, how.

**Findings:** Using *Arabidopsis thaliana* as a research system, we found that the *cryptochrome1* (*cry1*) mutant with an aberrant blue light receptor displays secondary cell wall defects in inflorescence stem fibers. Such defects were caused by inactivation of the NST1-directed transcriptional networks, which are involved in secondary cell wall formation in fiber cells. MYC2/MYC4, the expression of which is responsive to blue light, were able to directly bind to the *NST1* promoter and activate its transcriptional activity. Thus, blue light perceived by *CRY1* enhances cell wall thickening via *MYC2/MYC4* activation of the *NST1*-directed transcriptional network in Arabidopsis.

**Next steps:** Different wavelengths of light perceived by plants may cooperatively regulate secondary cell wall thickening. We are still working to understand the roles of other wavelengths of lights (such as red/far-red and UV light) in secondary cell wall formation. Our aim is to provide a comprehensive understanding of the light regulation of secondary cell wall formation.

(Wargent et al., 2009; Hectors et al., 2010; Robson et al., 2015). These observations imply that cell wall thickening is affected by different wavelengths of light. However, the underlying mechanism(s) is yet to be defined at the molecular level.

Arabidopsis *CRYPTOCHROME1* (*CRY1*) encodes a blue light receptor and plays a critical role in photomorphogenesis (Ahmad and Cashmore, 1993), affecting plant height, shade avoidance, apical meristem activity, root growth, seed size, and other phenotypes (Liu et al., 2011). CRY1 is located in both the nucleus and cytoplasm and interacts with other proteins to regulate a variety of plant developmental processes (Phee et al., 2007).

MYC2, a bHLH TF, is involved in a variety of regulatory processes such as root stem cell niche maintenance (Chen et al., 2011; Gasperini et al., 2015), seed protein accumulation (Gao et al., 2016), response to pathogens (Dombrecht et al., 2007; Fernández-Calvo et al., 2011; Kazan and Manners, 2013), and signaling by the hormones ethylene (Song et al., 2014; Zhang et al., 2014), gibberellic acid (Hong et al., 2012), and abscisic acid (Chen et al., 2012). In response to blue light, MYC2 is able to bind to the promoter of HYH and SPA1 to regulate photomorphogenesis (Gangappa et al., 2010; Maurya et al., 2015).

In this study, we report that CRY1 functions in the blue light enhancement of the SCW thickening of fiber cells in Arabidopsis inflorescence stems. In response to blue light, SCW thickening is enhanced, which is mediated by MYC2/MYC4 directly binding to the *NST1* promoter to activate the transcriptional regulatory network. These data reveal a molecular mechanism for the blue light regulation of SCW thickening in Arabidopsis fiber cells.

## RESULTS

### *CRY1* Plays a Role in Fiber Cell SCW Thickening in Arabidopsis

*Arabidopsis cry1* mutants are known to display phenotypic changes in photomorphogenesis (Ahmad and Cashmore, 1993). Here, we examined the *cry1* mutant for its inflorescence stem phenotypes. Compared with the wild type, the *cry1* mutant at the mature stage (10 weeks old) was taller, but *CRY1* overexpressing plants (*CRY1-OE*) displayed an opposite phenotype (Figures 1A and 1C). We recorded the growth of the inflorescence stem and found that in *cry1* the inflorescence stem grew faster and had a larger diameter than the wild type, whereas *CRY1-OE* plants were slower growing and had a smaller stem diameter (Figures 1B and 1D; Supplemental Figure 1A). Interfascicular fiber and xylem cells are major stem tissues supporting inflorescence upright growth. We examined the inflorescence stem structure and found that the fiber cells were longer with a larger diameter in the *cry1* mutant but shorter with a smaller diameter in *CRY1-OE* plants compared with those in the wild type (Figures 1E to 1H). Additionally, the *cry1* stem contained a similar number of interfascicular fiber cell layers as that in wild-type plants, whereas fewer layers of cells were present in *CRY1-OE* plants (Figures 1G and 1I). This suggests that *CRY1* plays a role in affecting fiber cell morphology. Further analysis of the fiber cell wall by TEM revealed that a thinner SCW was formed in *cry1* mutants, while a thicker SCW was deposited in *CRY1-OE*, compared with those in the wild type. This is consistent with the RT-qPCR analysis, which showed an expression increase of the SCW formation-related genes in the *CRY1-OE* plants (Supplemental Figure 1B). However, the vessel SCW thickness showed no significant differences between wild-type, *cry1*, and *CRY1-OE* plants (Figures 2A to 2C). The SCW thickness was also analyzed at an older stage (Figure 2C; Supplemental Figure 1C) and a similar pattern in SCW thickness between the wild-type, *cry1*, and *CRY1-OE* plants was observed. ANOVA indicated that the SCW thickness of fiber cells was affected by *CRY1* (Figure 2C).

Because CRY1 encodes a blue light receptor and plays a critical role in photomorphogenesis, we decided to examine the effects of blue light on SCW thickening in the inflorescence stem. We first grew wild-type, *cry1*, and *CRY1-OE* Arabidopsis plants in white light for ~3 weeks until bolting and then transferred them to a blue light growth chamber for inflorescence stem elongation. Inflorescence stems were collected when they reached 10 cm in length and cross sections in the basal region

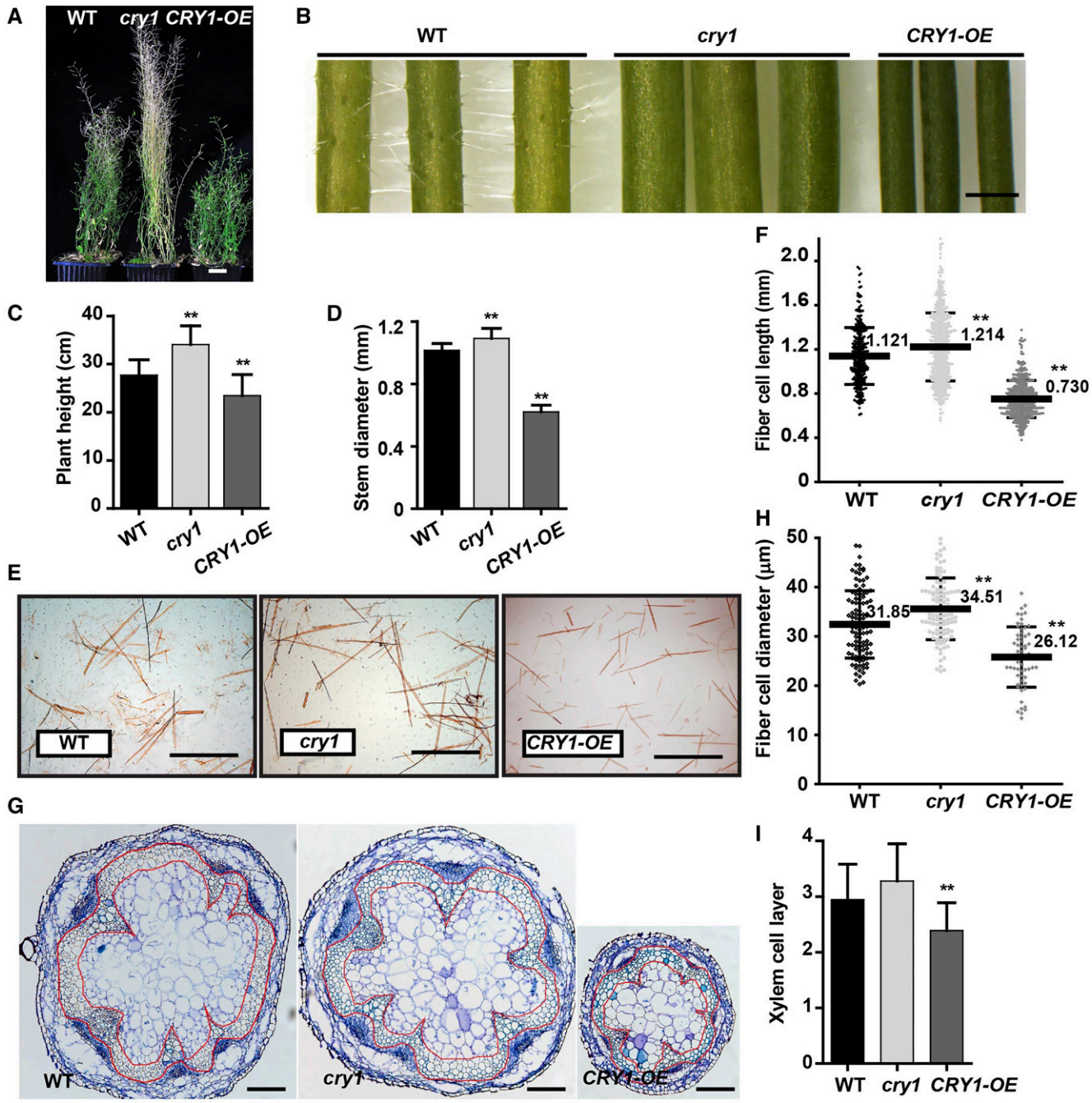


**Figure 1.** CRY1 Affects Elongation and Morphology of the Fiber Cells in Inflorescence Stems.

**(A)** Growth phenotypes of Arabidopsis plants after 10 weeks of growth in white light. Bar = 2 cm.

**(B)** Inflorescence stem (lower part). Bar = 1 mm.

**(C)** Heights of *cry1*, *CRY1* overexpression (*CRY1-OE*), and wild type (WT) plants. More than 20 plants per genotype were analyzed.

**(D)** Inflorescence stem diameter. More than 20 plants per genotype were analyzed. Student's *t* test (**P < 0.01) was used for statistical analyses; mean ± SD.

**(E)** Disaggregated fiber cells in **(B)** stained with Safranin T. Bar =1 mm.

**(F)** Fiber cell length. More than 500 fiber cells were measured in each sample and three biological replicates were performed. Student's *t* test (**P < 0.01) was used for statistical analyses; mean ± SD.

**(G)** Stem cross-sections stained with toluidine blue. Interfascicular fiber and xylem cells are shown within the area enclosed in the red markings. Bar = 200 μm.

**(H)** Fiber cell diameter. About 100 fiber cells were measured in each sample and three biological replicates were performed. Student's *t* test (**P < 0.01) was used for statistical analyses; mean ± SD.

**(I)** Layers of xylem cells in **(G)**. Three biological replicates and more than 15 samples ($n \geq 15$) from each genotype were analyzed. Student's *t* test (**P < 0.01) was used for statistical analyses; mean ± SD.

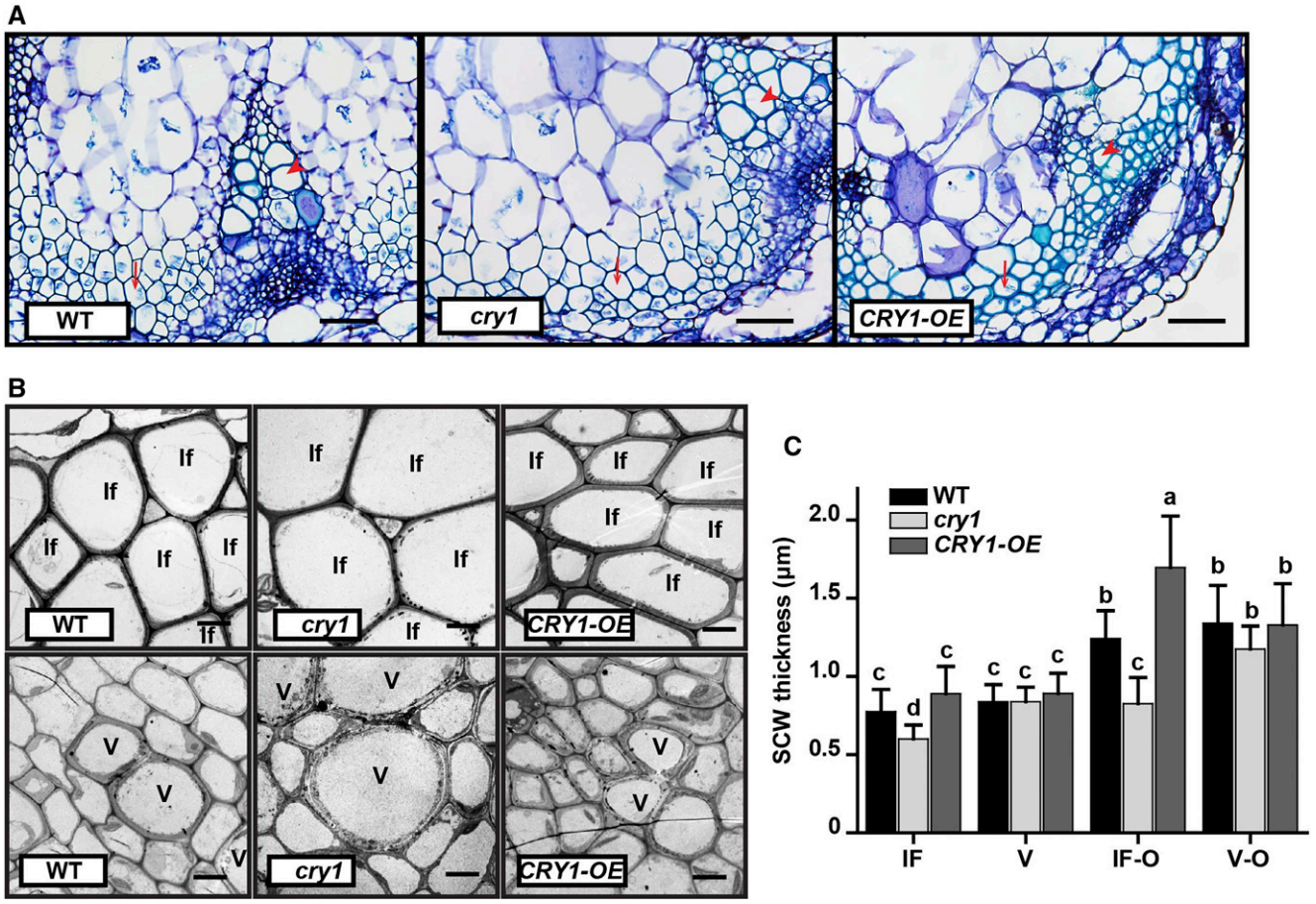


**Figure 2.** CRY1 Affects SCW Thickening in the Fiber Cells of Inflorescence Stems.

**(A)** Light micrographs of cross-sections of the inflorescence stem, stained with toluidine blue. Bar = 50 μm. Arrows, fiber cells; arrowheads, vessel cells.

**(B)** Transmission electron micrographs of the cross section of cells in **(A)**. Co, cortex; If, interfascicular fiber cell; V, vessel. Bar = 5 μm.

**(C)** Statistical analysis of SCW thickness in the interfascicular fiber cells and vessel cells in different developmental stages (Supplemental Figure 1C; IF-O and V-O). Three plants in each genotype and more than 20 cells in each plant were analyzed. Two-way ANOVA ($\alpha = 0.05$) was used to compare the genotype and development stage effect on SCW thickening. Mean ± SD.

IF, interfascicular fiber cell; V, vessel; IF-O, interfascicular fiber cell in another older stage; V-O, vessel in another older stage.

were analyzed. Compared with the wild type, *cry1* displayed a significant decrease in SCW thickness in fiber cells. Conversely, overexpression of CRY1 (*CRY1-OE*) significantly increased SCW thickness of fiber cells. Furthermore, the SCW thickness and morphology of vessel cells in *cry1* and *CRY1-OE* plants showed little difference compared with the wild type (Figures 3A to 3G). To test whether the CRY1 effect on SCW thickening is blue light specific, we compared inflorescence stems of plants grown under red light. We observed a similar SCW thickening in the inflorescence fiber and vessel cells between wild-type, *cry1*, and *CRY1-OE* plants (Supplemental Figures 2A to 2C). Furthermore, the expression of the SCW thickening-related genes was essentially the same between the wild-type, *cry1*, and *CRY1-OE* plants (Supplemental Figure 2D). Taken together, these data indicate that blue light plays a role in regulating SCW formation in the fiber cells of the inflorescence stem.

In Arabidopsis, both *NST1* and *SND1* are proposed to be the main TFs controlling SCW formation in fiber cells (Mitsuda et al., 2007; Zhong et al., 2007). The *snd1 nst1* double mutant displayed a lodging phenotype with little SCW thickening in fiber cells, while *NST1* overexpression (*NST1-OE*) resulted in a reduced growth rate and enhanced SCW thickening in fiber cells with ectopic lignin deposition in pith cells (Supplemental Figures 3A to 3D). Gene expression analyses revealed that the SCW thickening-related genes, such as the TF *MYB46* and the lignin biosynthesis gene *4CL1* were upregulated in *NST1-OE* plants and downregulated in the *snd1 nst1* double mutant (Supplemental Figure 3E). Measurement of the inflorescence stem tensile strength revealed that the mechanical strength increased drastically in *NST1-OE* plants but decreased substantially in the *snd1 nst1* double mutant (Supplemental Figure 3F), suggesting a strong positive association between stem tensile strength and

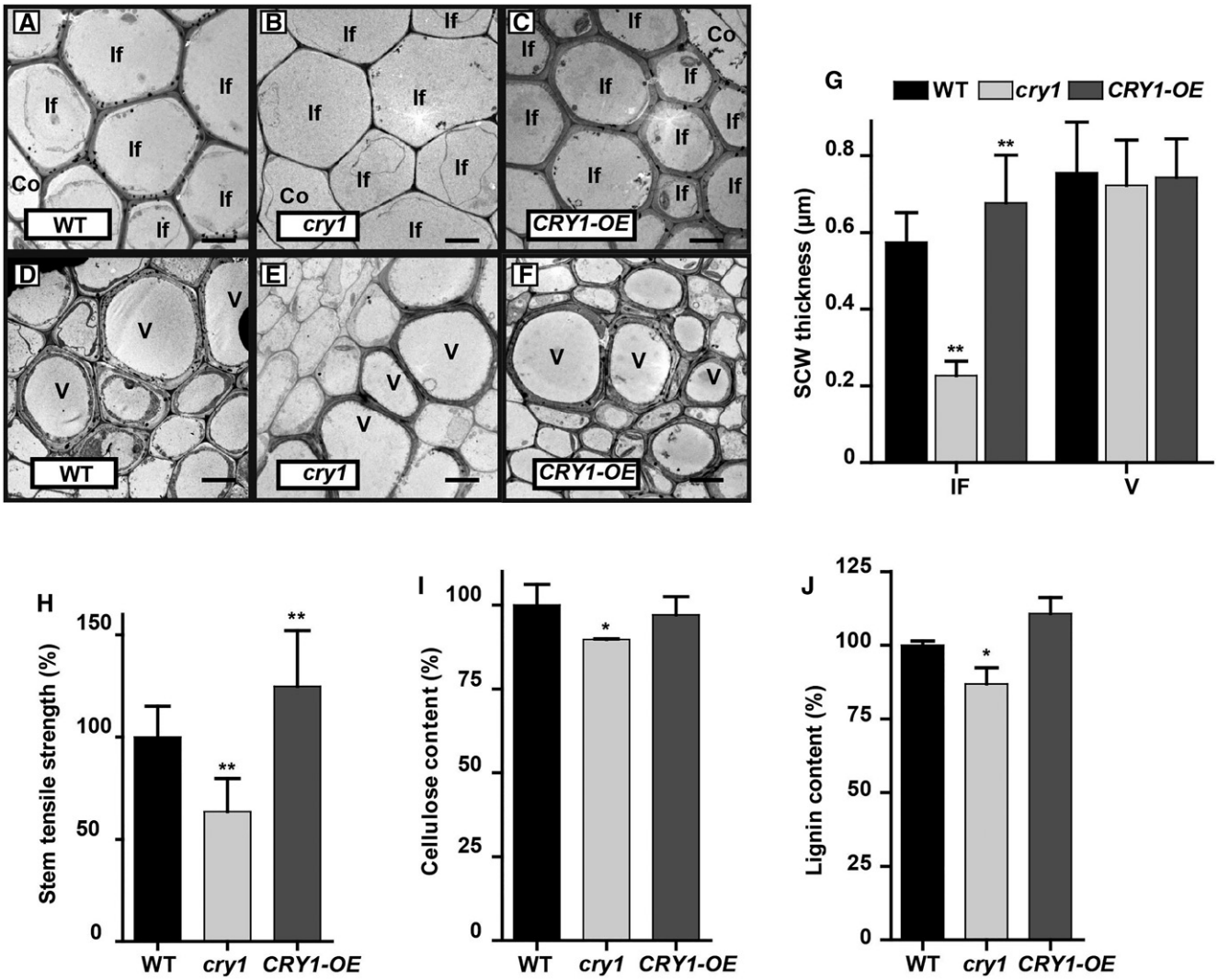


**Figure 3.** CRY1 Positively Regulates SCW Thickening in Fiber Cells, but Not Vessels in Blue Light.

**(A)** to **(F)** Transmission electron micrographs of the cross section of the inflorescence stem grown in blue light. Interfascicular fiber cells ([**A] to [C]**) and vessels ([**D] to [F]**). Co, cortex; If, interfascicular fiber cell; V, vessel. Bar = 5 μm.

**(G)** Measurements of SCW thickness in **(A)** to **(F)**. Three plants in each genotype and more than 20 cells in each plant were analyzed; mean ± SD.

**(H)** Tensile strength measurements of the inflorescence stem. More than 20 plants in each genotype were analyzed; mean ± SD.

**(I)** and **(J)** SCW components in the inflorescence stem. Content of cellulose **(I)** and lignin **(J)**. Three biological repeats were performed. Student's *t* test (**P < 0.01) was used for statistical analyses; mean ± SD.

fiber cell SCW thickness. Similarly, the inflorescence stem tensile strength was dramatically lower in the *cry1* mutant but significantly higher in the *CRY1-OE* plants than in wild-type plants (Figure 3H). Furthermore, determination of cell wall composition indicated that lignin content of SCW was lower in the *cry1* mutant but higher in *CRY1-OE* plants than in the wild type. The other two major macromolecular components, including cellulose and noncellulosic polysaccharides, were also altered accordingly in the *cry1* mutant and *CRY1-OE* plants (Figures 3I and 3J; Supplemental Figure 4). These results further confirmed that a blue light signal is involved in regulating SCW biosynthesis in fiber cells during inflorescence stem growth.

### The Transcription Program for SCW Formation Is Suppressed in the *cry1* Mutant

To investigate how blue light plays a role in SCW formation of fiber cells, we conducted RNA-seq analysis of the inflorescence stems of wild-type and *cry1* plants grown in blue light. Compared with the wild type, a group of 612 differentially expressed genes (DEGs) (adjusted P value < 0.01) were detected in the inflorescence stem of *cry1* mutant plants. Gene Ontology (GO) analysis showed that the DEGs were significantly enriched in genes associated with cell wall-related processes (Figure 4A). Among them, expression of the SCW formation genes, including

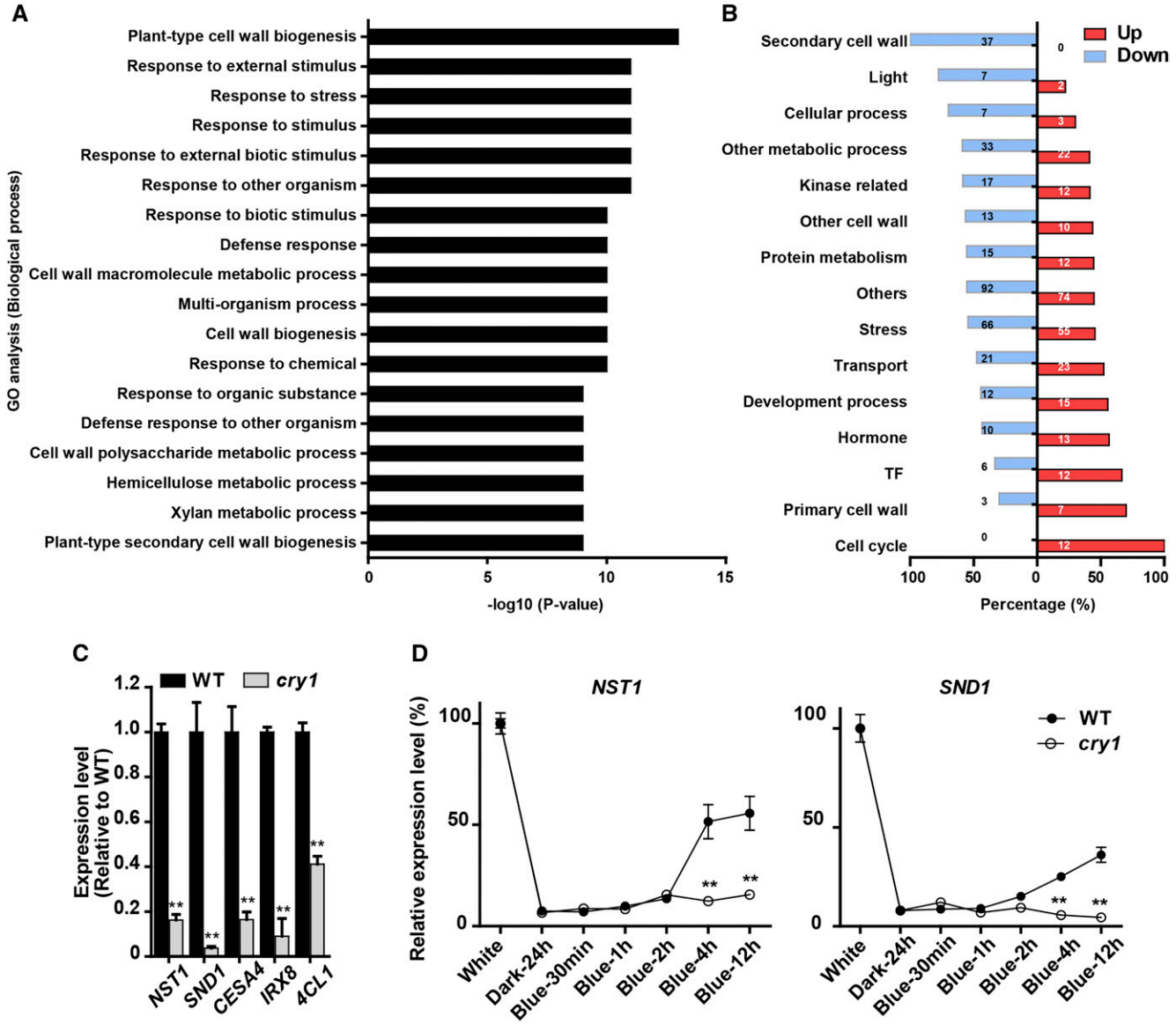


**Figure 4.** CRY1 Regulates the Expression of the SCW Formation-Related Genes in Blue Light.

**(A)** GO enrichment analysis of the DEGs in the inflorescence stem of *cry1* relative to the wild type. The GO terms of biological processes with statistical significance (P value ≤ e-09) are shown. Three biological replicates were performed for each genotype.
**(B)** Percentage of up- and downregulated genes in *cry1* within different functional categories. Bar plot shows the percentage of downregulated (gray)/upregulated (black) genes in each category. The number in each box indicates the number of DEGs.
**(C)** Quantitative RT-PCR confirmation of the effect of CRY1 on the expression of the SCW-related genes (*NST1*, *SND1*, *CESA4*, *IRX8*, and *4CL1*). Three biological repeats were performed. Student's *t* test (**P < 0.01) was used for statistical analysis; mean ± SD.
**(D)** Induction of *NST1* (left) and *SND1* (right) expression by blue light. Arabidopsis plants (5 weeks old) were transferred to darkness for 24 h to silence expression of the light-induced genes. Then the plants were treated with blue light to detect the induction of gene expression in the inflorescence stem. Three biological repeats were performed. Student's *t* test (**P < 0.01) was used for statistical analyses; mean ± SD.

several key TF regulatory genes was decreased (Figure 4B; Supplemental Data Set 1). RT-qPCR analysis further confirmed that the expression of *NST1*, *SND1*, *CESA4* (Taylor et al., 2003), *IRX8* (Hao et al., 2014), and *4CL1* (Lee et al., 1997), which are all involved in the formation of SCW polysaccharides and lignin, were suppressed in the *cry1* mutant (Figure 4C). This suggests that *CRY1* is involved in regulating the transcription of SCW formation in inflorescence stems.

We then examined the spatio-temporal pattern of *CRY1* expression. *CRY1* was ubiquitously and highly expressed in various

tissues such as the leaf, stem, and silique (Supplemental Figure 5A). Immunohistochemical analyses show that CRY1 was found in interfascicular fibers and xylem fiber cells (Supplemental Figure 5B). This indicates that *CRY1* is expressed in the fiber cells undergoing SCW formation.

These data suggested that a blue light signal may be involved in regulating the SCW transcriptional network. This prompted us to investigate whether *NST1* and *SND1* are regulated by blue light in Arabidopsis, as they are believed to be the main TF genes for initiation of the transcriptional network for SCW formation (Mitsuda et al., 2007; Zhong et al., 2007). We first grew *cry1* and wild-type Arabidopsis plants for 5 weeks and transferred them to darkness for 24 h to silence the expression of the light-induced genes. Then, the plants were transferred to blue light to examine the changes in gene expression induced by blue light over a 12-h period. Both *NST1* and *SND1* expression were responsive to blue light but the induction of *NST1* expression was faster and greater. However, in *cry1* plants, neither *NST1* nor *SND1* responded to blue light induction (Figure 4D). These results indicate that expression of both *NST1* and *SND1* was upregulated by blue light through CRY1.

### MYC2/MYC4 Bind to the *NST1* Promoter Directly

To examine how *NST1* expression is regulated by the blue light signal, we cloned the *NST1* promoter and utilized yeast one-hybrid (Y1H) screening to search for the possible factor(s) responsive to the blue light signal and activates *NST1* transcription. The 3.7-kb *NST1* promoter was arbitrarily divided into eight fragments to construct the Y1H screening system (Supplemental Figure 6A). By Y1H screening, ~1200 positive clones were selected from the cDNA library of Arabidopsis wild-type florescence stem and sequenced. Ten candidate genes that appeared at least twice within the selected clones were selected for further characterization. Among them, *MYC2* and *PHL2* appeared more than 40 times (Supplemental Table 1). Four genes, *PHL2*, *HB30*, *MYC2*, and *MYC4*, were then verified for their binding activity in the Y1H bait cells (Supplemental Table 1).

To test whether these genes are involved in SCW thickening, we examined their expression patterns. *PHL2* and *HB30* showed relatively low expression in the rosette leaves, stem, and root, but both were highly expressed in the flower, silique, and the tip of the inflorescence stem (Supplemental Figure 6B). *MYC2* was highly expressed in a variety of tissues including roots and stems. *MYC4* showed a preference for expression in stems, flowers, and siliques. We also examined whether these genes were responsive to blue light and found that expression of both *MYC2* and *MYC4* was rapidly induced by blue light and dependent on *CRY1* (Figures 5A and 5B). Next, we divided MYC2 and MYC4 into several fragments to investigate which part is able to bind to the *NST1* promoter in the Y1H assay. MYC2 with a C-terminal fragment from 445 to 623 amino acid residues and MYC4 with a C-terminal fragment from 360 to 589 amino acid residues were able to bind to the *NST1* promoter (Supplemental Figures 7A and 7B).

To assess whether *MYC2* and *MYC4* can activate *NST1* expression, we conducted a dual-luciferase (LUC) reporter assay in Arabidopsis protoplasts. Coexpression of either *MYC2* or *MYC4* with LUC driven by the *NST1* promoter resulted in a significant increase in luminescence signal, indicating that both MYC2 and MYC4 were able to activate the *NST1* promoter (Figure 5C). In addition, fusion of the VP16 transactivation domain with the MYC2 C-terminal binding fragment, but not the N-terminal fragment was also able to activate *NST1* expression (Figure 5C). Next, the 3.7-kb *NST1* promoter was fragmented for MYC2 activation analysis in Arabidopsis protoplasts. Analyses revealed that two regions on the *NST1* promoter located between –2208 to ~–2674 and –453 to ~–1309 from the initiating ATG were responsible for MYC2 binding (Supplemental Figure 7C).

For further in vivo verification, we performed a chromatin immunoprecipitation (ChIP) assay by generating transformants with integration of *35S-MYC2-3FLAG* or *35S-MYC4-3HA* in Arabidopsis. The complex of protein and DNA fragments was prepared from the inflorescence stem of the transgenic plants and immunoprecipitation was performed using FLAG and HA antibodies, respectively (Supplemental Figure 7D). A strong enrichment of two DNA fragments from the *NST1* promoter located between –904 to ~–1103 (F3) and –2470 to ~–2675 (F1) was detected (Figure 5D). The sequences of the two fragments matched the binding regions identified by promoter deletion analysis (Supplemental Figure 7C). As a positive control for MYC2 binding, the *EIN3 BINDING F-BOX PROTEIN1* promoter fragment (–1188 to ~–1388; Zhang et al., 2014) was also detected in the immunoprecipitations (Supplemental Figure 7E). Thus, both in vitro and in vivo evidence demonstrated that MYC2 and MYC4 bind directly to the *NST1* promoter and activate *NST1* expression.

### *MYC2* and *MYC4* Respond to Blue Light and Function Downstream of *CRY1*

To investigate how MYC2/MYC4 function in the response to blue light, a *myc2 myc4* double mutant was crossed with both the *cry1* mutant and *CRY1-OE* plants. Compared with wild-type plants, the *CRY1-OE* plants displayed a similar rosette leaf number and flowering time (Supplemental Figure 8) (Lin, 2000b) but shortened inflorescence stem (Figure 6A; Supplemental Figure 1A). The *CRY1-OE* inflorescence stem phenotype was partly restored in *CRY1-OE myc2 myc4* plants (Figure 6A). Expression of the SCW formation-related genes such as *NST1*, *4CL1*, and *IRX8* was lower in *CRY1-OE myc2 myc4* plants than in *CRY1-OE* plants (Figure 6B). By contrast, in *cry1 myc2 myc4* triple mutant plants, the phenotypes and SCW formation-related gene expression remained essentially unchanged compared with their parent plants (Figures 6A and 6C). On the other hand, overexpression of *MYC4* in the *cry1* mutant background was able to restore the expression of the SCW formation-related genes (Figures 6D and 6E). Furthermore, hypocotyl elongation, which was inhibited in *CRY1-OE* (Sang et al., 2005) (Supplemental Figures 8C and 8D), was normal in *CRY1-OE myc2 myc4* plants (Supplemental Figures 8C and 8D). The CRY1 protein level in *CRY1-OE myc2 myc4* plants was lower than in *CRY1-OE* plants (Supplemental Figure 8A). The *CRY1-OE* and *CRY1-OE myc2 myc4* lines should have the same amount of CRY1 protein if no silencing occurs. One possibility is that the *myc2 myc4* double mutant has reduced CRY1 protein levels; further work is needed to test this possibility.

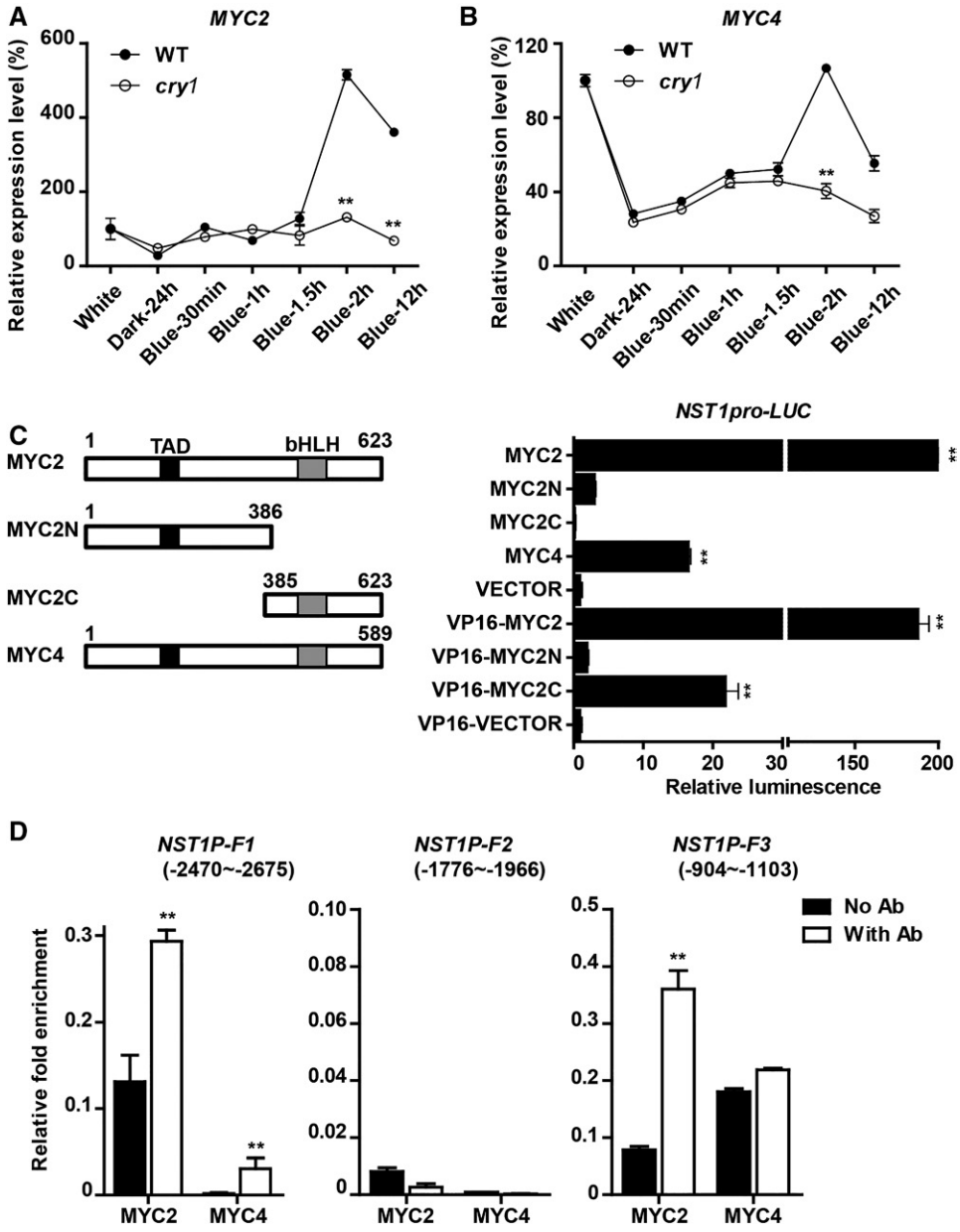


**Figure 5.** MYC2 and MYC4 Directly Bind to the *NST1* Promoter.

**(A)** and **(B)** Blue light induction of *MYC2* and *MYC4* expression, respectively. Arabidopsis plants (5 weeks old) were transferred to darkness for 24 h to silence expression of the light-induced genes. Then the plants were treated with blue light to examine the blue light induction of *MYC2* and *MYC4* expression in the inflorescence stem.

**(C)** Activation of the *NST1* promoter by MYC2/MYC4. Left: Schematic diagram of MYC2 and MYC4 structure with amino acid lengths and the TAD and bHLH domains indicated. Right: Activation activities. Transactivation assays were performed through cotransformation of mesophyll protoplasts of Arabidopsis with *pGreenII0800-NST1*$_{pro}$ and *pA7-35S-MYC2/4* constructs. VP16 is a transcriptional activator derived from herpes simplex virus protein. Three biological repeats were performed.

**(D)** ChIP analysis of MYC2 and MYC4 binding to the *NST1* promoter fragments. Transgenic T2 Arabidopsis (4 weeks old) plants overexpressing *MYC2* or *MYC4* were analyzed. *NST1P-F1*, *NST1P-F2*, and *NST1P-F3* represent three fragments of the *NST1* promoter. Student's *t* test (**P < 0.01) was used for statistical analyses; mean ± SD.

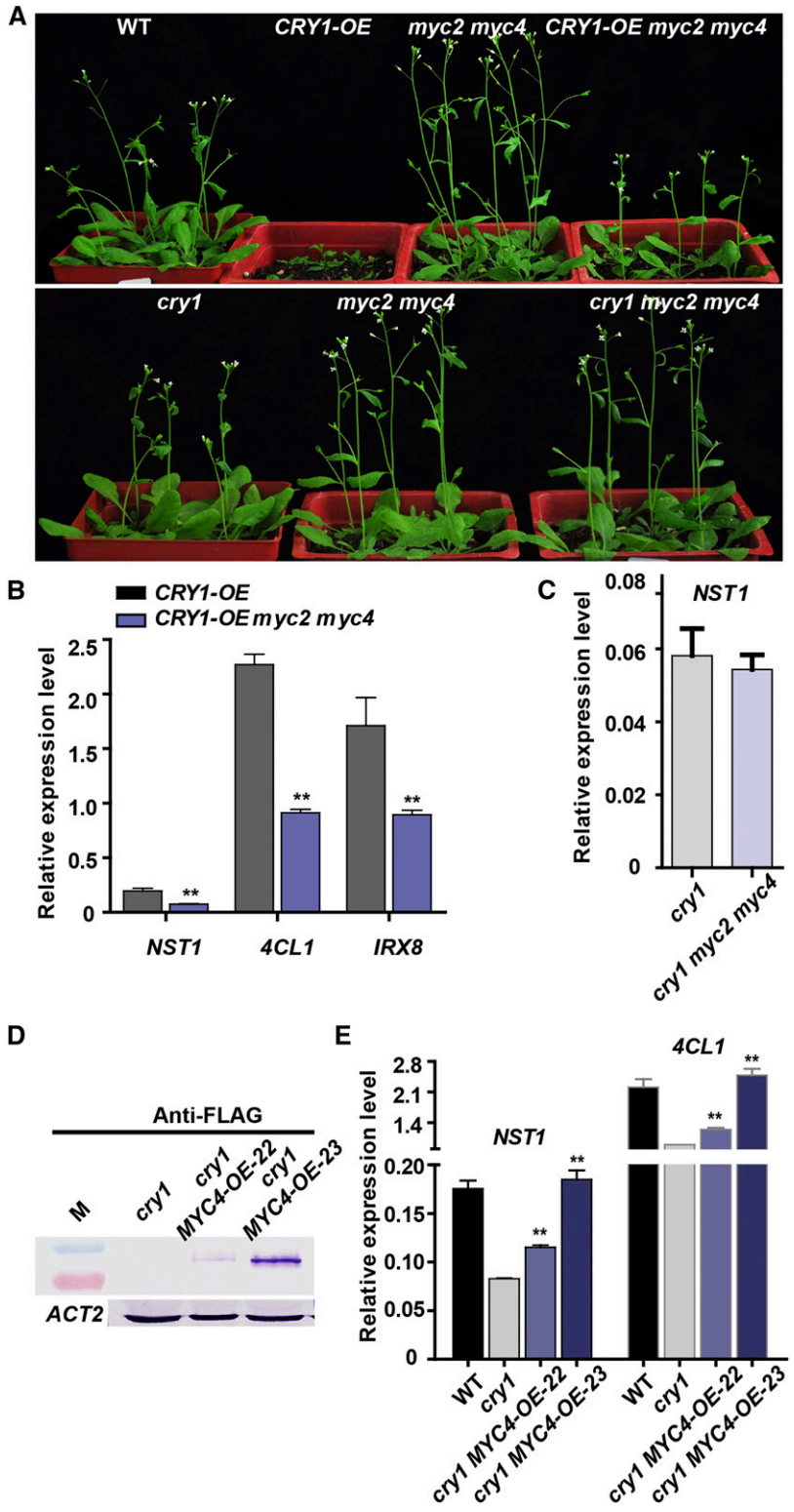


**Figure 6.** *MYC2* Genetically Interacts with *CRY1*.

**(A)** Arabidopsis wild type (WT) and mutant/transgenic (CRY1-OE; *myc2 myc4*; CRY1-OE *myc2 myc4*) plants (4 weeks old).
**(B)**, **(C)**, and **(E)** Expression of the key SCW formation-related genes in *myc2* and *cry1* mutant plants. Student's *t* test (**P < 0.01) was used for statistical analysis; mean ± SD. Three biological repeats were performed.
**(D)** Immunoblot detection of MYC4 protein in the *cry1* mutant overexpressing *MYC4*. ACTIN2 was used as an internal control.

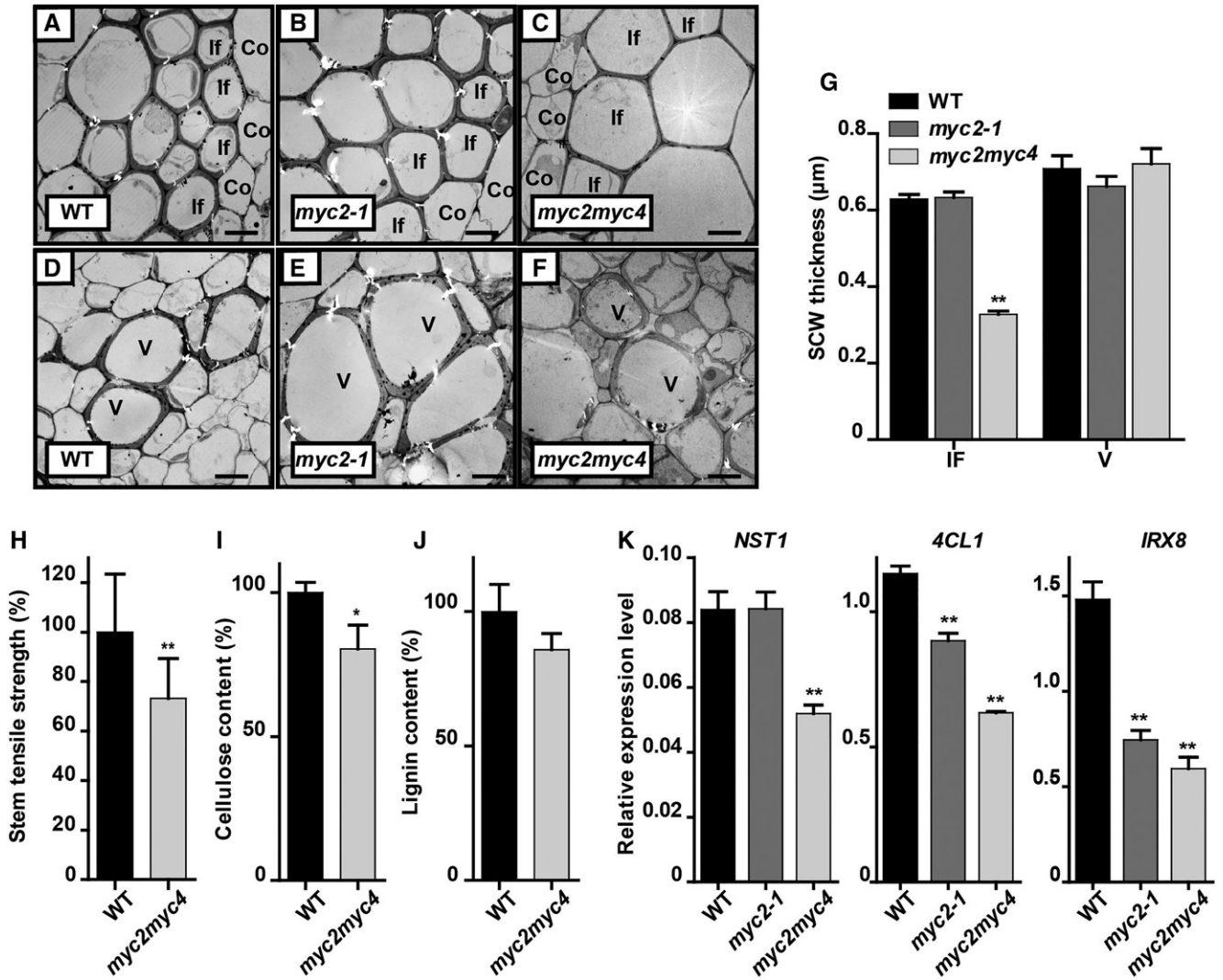


**Figure 7.** MYC2 and MYC4 Positively Regulate SCW Formation in Fiber Cells under Blue Light.

**(A)** to **(F)** Transmission electron micrographs of the cross sections of *myc2* and *myc2 myc4* inflorescence stems grown in blue light. Co, cortex; If, interfascicular fiber cell; V, vessel. Bar = 5 μm.

**(G)** Measurements of SCW thickness of interfascicular fiber cells and vessel cells in **(A)** to **(F)**. Three plants per genotype and more than 20 cells were analyzed. Student's *t* test (**P < 0.01) was used for statistical analyses; mean ± SD.

**(H)** Tensile strength measurements of the inflorescence stem grown in blue light. More than 20 plants were analyzed, Student's *t* test (**P < 0.01) was used for statistical analyses; mean ± SD.

**(I)** and **(J)** Relative content of lignin **(I)** and cellulose **(J)** in the same stem region as **(H)**. Three biological repeats were performed. Student's *t* test (*P < 0.1) was used for statistical analyses; mean ± SD.

**(K)** Expression of the SCW-related genes (*NST1*, *4CL*, and *IRX8*) in the same stem region as **(H)**. Three biological repeats were performed. Student's *t* test (**P < 0.01) was used for statistical analyses; mean ± SD.

Nevertheless, the results presented here demonstrate that both *MYC2* and *MYC4* genetically interact with *CRY1* and function downstream of *CRY1*.

### MYC2 and MYC4 Positively Regulate SCW Thickening under Blue Light

To determine whether *MYC2* and *MYC4* regulate SCW thickening, we first examined their tissue expression patterns. Promoter-GUS analysis revealed that *MYC2* and *MYC4* show similar expression patterns in leaf veins and specifically in the interfascicular fibers and xylem cells, with little signal in vessel cells (Supplemental Figure 9). Thus, expression of *MYC2* and *MYC4* in the vascular system was associated with SCW thickening.

To confirm that *MYC2* and *MYC4* function in SCW thickening, we measured the SCW thickness in the stem of *myc2* and *myc2 myc4* mutant plants. The SCW thickness was substantially

reduced in fiber cells in *myc2 myc4* double mutants but was relatively unchanged in the *myc2* single mutant, and the vessel cells showed no change in thickness in either the *myc2* or *myc2 myc4* mutants (Figures 7A to 7G). These results suggest that *MYC2* and *MYC4* act cooperatively to regulate SCW thickening of fiber cells in plants grown in blue light.

To examine the effect of *MYC2* and *MYC4* on the properties of the thickened SCW, we measured the tensile strength of the *myc2 myc4* double mutant inflorescence stem and showed, as predicted, that it was decreased significantly compared with wild-type plants (Figure 7H). These data also in accordance with the reduced levels of both lignin and cellulose in the *myc2 myc4* double mutant (Figures 7I and 7J) as well as the content of noncellulosic polysaccharides that mirrored those previously observed in the *cry1* mutants (Supplemental Figure 10). Expression of *NST1*, *4CL1*, and *IRX8* was also decreased significantly in the *myc2 myc4* double mutant, but was only slightly affected in the *myc2-1* mutant (Figure 7K). Overexpression of *MYC2* led to increased expression of *NST1*, *IRX8*, and *4CL1* in Arabidopsis inflorescence stem (Supplemental Figure 11). These results indicated that both *MYC2* and *MYC4* positively regulate fiber SCW thickening.

## DISCUSSION

Higher plants develop cells with thickened secondary cell wall in vascular tissue which equip plants with mechanical strength and long-distance conducting capacity for erect growth (Lucas et al., 2013). Indeed, most of the photosynthetic carbon fixed by higher plants is transformed into polysaccharides and lignin deposited in SCWs, providing human society with indispensable renewable biomass resources (Kumar et al., 2016). SCW formation is regulated by various developmental and environmental signals. However, how the environmental signals regulate SCW thickening is poorly understood. In this study, we report that CRY1 mediates blue light promotion of SCW thickening in the fiber cell of Arabidopsis.

### Blue Light Enhances Fiber Cell SCW Thickening

In Arabidopsis, blue light inhibits hypocotyl growth (Sellaro et al., 2010). In response to blue light depletion, elongation of the hypocotyl, internode, stem, and petiole is enhanced (Keller et al., 2011). During hypocotyl growth, cell elongation, which involves primary cell wall modification, determines the hypocotyl length. RNA-seq analysis showed that the expression of genes involved in primary cell wall modification, such as *XTH15* and *XTH17* (Sasidharan et al., 2010), are upregulated in blue light-grown *cry1* mutant (Supplemental Data Set 1), indicating that blue light may play a role in inhibiting cell elongation through regulating primary cell wall modification. However, in vascular cells, cell elongation of primary cell walls and SCW formation need to be coordinated. Usually, SCW formation occurs after cell elongation stops and is precisely regulated in a spatio-temporal manner (Taylor-Teeples et al., 2015). During growth of the Arabidopsis inflorescence stem, our study showed that SCW thickening is enhanced and the transcriptional regulatory program for SCW biosynthesis (Mitsuda et al., 2007; Zhong et al., 2007; Hussey et al., 2013; Schuetz et al., 2013) is upregulated in response to a blue light signal. Genetic analyses revealed that the Arabidopsis *cry1* mutant shows longer fiber cells with thinner cell walls, while *CRY1* overexpression decreased fiber cell length and increased cell wall thickness (Figures 1 and 2). These data indicated that blue light promotes SCW thickening in fiber cells. Consistent with the blue light effect on inhibiting hypocotyl growth (primary cell wall formation during cell expansion), evidence suggests that blue light enhances SCW formation in the vasculature. On the other hand, the red/far red light receptor PHYTOCHROME B (PHYB) may also play a role in cell wall formation. The *phyb* mutant displays increased cell elongation, and elongated hypocotyls and inflorescence stem (Reed et al., 1993). Activation of PHYB was able to affect the cellulose synthesis in the primary cell wall (Bischoff et al., 2011). It is unclear at this time how PHYB interacts with CRY1 to regulate cell wall formation.

Immunohistochemical analysis revealed CRY1 accumulation in fiber cells; however, it remains to be determined whether the SCW regulation by blue light is cell-autonomous or occurs through a mobile signal. Blue light may penetrate the epidermis to reach inner cell layers (Koning, 1994), thereby triggering CRY1 signaling in fiber cells; however, in the case of PHYB signaling, both stem light sensing and a possible mobile signal have been reported (Kim et al., 2016; Lee et al., 2016), suggesting there may be other explanations.

Interestingly, we found that CRY1 affects SCW thickening in fiber cells but not in vessel cells. In the development of the

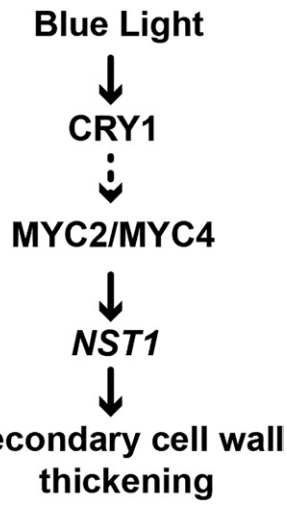


**Figure 8.** A Proposed Model of Blue Light Regulation of SCW Thickening in Arabidopsis.

Blue light enhances SCW thickening in fiber cells of the inflorescence stem. When CRY1 perceives blue light, it can upregulate the expression of *MYC2* and *MYC4*. Binding of MYC2 and MYC4 to the *NST1* promoter leads to activation of the SCW formation-related transcriptional program for enhancement of SCW thickening. Arrows: A direct regulation or interaction that has been confirmed by experiments. Dashed arrow: An interaction has been suggested by the mechanism.

vasculature, vessel and fiber cells are differentiated from the procambium to perform different functions (Caño-Delgado et al., 2010). This process is coordinated through a complex array of signaling molecules/processes (that are not fully elucidated) that control the differentiation into vessel and fiber cell types (Ruonala et al., 2017). SCW thickening in vessel and fiber cells is known to be activated by different TFs, VND6/VND7 in vessels (Yamaguchi et al., 2008; Zhong et al., 2008), and SND1/NST1 in fibers (Zhong et al., 2006; Mitsuda et al., 2007), even though they may share some downstream targets of SCW thickening (Schuetz et al., 2013). In response to blue light, *NST1* expression is upregulated for enhancement of SCW thickening in a fiber cell-specific manner.

### MYC2/MYC4 Respond to the Blue Light Signal and Enhance Fiber Cell SCW Thickening

MYC2 is a versatile TF that participates in many different cellular processes by interconnecting a variety of endogenous and exogenous signals that regulate plant growth and development (Kazan and Manners, 2013). In response to blue light, *MYC2* is involved in photomorphogenesis (Yadav et al., 2005). In this study, we found that *MYC2* expression is stimulated by blue light and is involved in regulating fiber SCW thickening in Arabidopsis inflorescence stems. Induction of *MYC2* by blue light is diminished in *cry1* mutants (Figure 5), indicating that CRY1 functions in the blue light induction of *MYC2*. Since MYC2 activity is also reported to be modulated under blue light in the hypocotyls of Arabidopsis seedlings (Sethi et al., 2014), it will be interesting to establish the mechanism by which blue light regulates the MYC2 and CRY1 proteins that in turn control the pathways leading to SCW thickening in the inflorescence stem of Arabidopsis. Overexpression of *MYC2* caused an increase in the transcriptional program underlying SCW biosynthesis (Supplemental Figure 11). Thus, enhancement of SCW formation by blue light may be mediated by *MYC2*. Additional analyses revealed that *myc2 myc4* and *cry1* mutants formed thinner fiber SCWs, but *CRY1-OE* plants produced thickened walls in fiber cells relative to the wild type. However, mutation of *myc2 myc4* in *CRY1-OE* plants decreased the SCW-related transcriptional program (Figure 6). These data suggest that both *MYC2* and *MYC4* mediate the blue light enhancement of SCW thickening in the Arabidopsis inflorescence stem. Since MYC2/MYC4 can interconnect a variety of endogenous and exogenous signals (Kazan and Manners, 2013), future research/experimentation will explore which of these signals function in controlling SCW thickening during development.

### MYC2/MYC4 Directly Bind to *NST1* Promoter to Fine-Tune the Transcriptional Regulatory Networks for SCW Thickening under Blue Light

MYC2 and MYC4 belong to the bHLH TF family, and members of this family bind to either G-box or related motifs (Dombrecht et al., 2007; Fernández-Calvo et al., 2011). In this study, analysis of the MYC2 binding site on the *NST1* promoter revealed the existence of several G-box motifs and our in vitro and in vivo results demonstrated that MYC2 and MYC4 can directly bind to the *NST1* promoter (Figure 5C; Supplemental Figure 7). This suggests a role for MYC2 and MYC4 in regulating the *NST1*-directed transcriptional program for SCW formation. Arabidopsis has several MYC TFs with high sequence similarity, such as MYC2, MYC3, MYC4, and MYC5, that function redundantly in the jasmonic acid signaling pathway and in stamen development (Kazan and Manners, 2013; Figueroa and Browse, 2015; Qi et al., 2015). In response to blue light, expression of both *MYC2* and *MYC4* was enhanced, which in turn promoted SCW thickening of fiber cells in the inflorescence stem of Arabidopsis. The double mutant *myc2 myc4* displayed thinner SCWs in fiber cells, while the *myc2* mutant did not show a significant effect on the SCWs of fiber cells (Figure 7). It is therefore likely that *MYC2* and *MYC4* and possibly other MYC TFs act redundantly to increase SCW thickening in response to blue light.

Blue light that is perceived by the blue light receptor CRY1 has been shown to affect plant height, shade avoidance, apical meristem activity, root growth, seed size, and other developmental processes (Liu et al., 2011). In addition to CRY1, the related blue light receptor CRY2 is reported to function in the control of flowering time, is circadian clock regulated (Lin et al., 1998; Liu et al., 2008), and is also involved in regulating hypocotyl elongation, in a manner that is redundant to CRY1 (Lin, 2000a). However, due to the late flowering of the *cry1 cry2* double mutant (Li et al., 2011), we were unable to analyze the inflorescence stem SCWs at the same growth stage under long-day conditions. Since *cry1* mutant plants show a SCW thickening phenotype in the inflorescence stem, it would be interesting to examine whether CRY2 is also involved in regulating SCW thickening.

Through the entire course of plant development, cell wall formation and modification shape the cellular structure for plant tissue differentiation and morphogenesis. It is conceivable that establishment of the plant body structure is tightly associated with the process of cell wall formation. Depletion of blue light stimulates elongation of internodes and petioles that is accompanied by upregulation of *XTH15* and *XTH17* for cell wall modification (Sasidharan et al., 2010; Keller et al., 2011; Keuskamp et al., 2011). In this study, we found that blue light enhanced SCW thickening but inhibited cell elongation in inflorescence stem fibers. This indicated that blue light is involved in cell wall modification and formation. As illustrated in Figure 8, the blue light signal perceived by CRY1 is able to induce expression of *MYC2* and *MYC4*, which in turn act as transcriptional activators that directly bind to the *NST1* promoter and stimulate the transcriptional program for SCW thickening. In conclusion, our findings reveal a molecular mechanism underlying the blue light enhancement of fiber SCW thickening in inflorescence stems.

## METHODS

### Plant Materials and Growth Conditions

*Arabidopsis thaliana* (Columbia-0) was grown in a phytotron with a light (fluorescent lamp, 80 μE/s*m$^2$)/dark cycle of 16 h/8 h at 22°C. The *cry1* and *CRY1-OE* (*MYC-CRY1*) plants were described previously (Sang et al., 2005). The *myc2-1* mutant (SALK_040500) and *snd1 nst1* (CS67921)

double mutant was ordered from the ABRC, and the *myc2 myc4* mutant (Song et al., 2014) was a kind gift from Daoxin Xie. The higher-order mutants were generated by genetic crosses using standard techniques, and genotyping was performed by PCR identification (Yeasen 2×Hieff PCR Master Mix, catalog no. 10102) of the T-DNA insertion (*MYC2* and *MYC4*) or gene length (*CRY1*) and by immunoblot analysis (CRY1-OE, anti-MYC from Abmart, catalog no. M20002L). *cry1 MYC4-OE* was generated by transformation of *p1300-35Spro-MYC4-3Flag* into the *cry1* mutant, and *NST1-OE* and *MYC2-OE* plants were generated by transformation of wild-type Arabidopsis with *p1300-4CL1$_{pro}$-NST1-3FLAG* and *p1300-35S$_{pro}$-MYC2-3Flag*, respectively. The *4CL1$_{pro}$* (–1 to ~–1633 from ATG) was PCR amplified from Arabidopsis genome, and protein overexpression was detected by immunoblot analysis (anti-FLAG from Abmart, catalog no. M20008L). Blue light treatment was performed when plants initiated bolting and the inflorescence stem started elongating. Blue light conditions were achieved using an LED light incubator (Percival E30LED; blue light wavelength = 470 nm, light intensity = 40 μE/s*m$^2$). Red light conditions were achieved using an LED light incubator (Percival E30LED; red light wavelength = 670 nm, light intense = 40 μE/s*m2). Briefly, Arabidopsis inflorescence stems that had reached 10 cm in length were used for analysis unless otherwise stated. *Agrobacterium tumefaciens*-mediated transformation was performed following the floral dip method (Clough and Bent, 1998).

### Quantitative RT-PCR Analysis

Total RNA was isolated from various tissues using the Promega kit. Total RNA was used for first-strand cDNA synthesis and then for qPCR analysis of transcript abundance. qPCR was performed using SYBR GreenMaster Mix (Bio-Rad; iTaq Universal SYBR Green Supermix, catalog no. 1725124) and an iQ5 Real-Time PCR detection system (Bio-Rad). Gene expression was normalized using *ACT2* as an internal control.

### RNA-Seq Analysis

For RNA-seq, wild-type (Col-0) and *cry1* mutant plants were grown in white light until bolting and then transferred to blue light for inflorescence stem elongation. The inflorescence stems of three independent plants of each genotype were collected, and total RNA from each plant was extracted for transcriptome sequencing. Sequencing and data analyses were conducted by The Beijing Genomics Institute using BGISEQ-500 using a well-developed bioinformatics pipeline (Mortazavi et al., 2008; Wang et al., 2009). Briefly, RNA-seq raw reads were filtered to remove the adaptor sequences and low-quality reads, and the resultant clean reads were aligned to the TAIR10 Arabidopsis genome by Bowtie2 (version v2.2.5) (Langmead et al., 2009) implemented by the HISAT2 program (version v2.0.4) (Kim et al., 2015). Next, gene expression level, FPKM (reads per kilobase of exon model per million mapped reads), was quantified and calculated by RSEM (version v1.2.12) (Li and Dewey, 2011). DEGs were identified by the NOISeq method (Tarazona et al., 2011) using the criterion of fold change ≥2 and divergence probability ≥0.8. For GO enrichment analysis, GO::TermFinder (Boyle et al., 2004) was used to associate DEGs and GO annotations and calculate enrichment significance. The calculated P value was adjusted by the Bonferroni correction method. Based on the GO analysis and gene function description on TAIR, the genes that were misregulated in *cry1* mutants grown under blue light were trimmed, annotated, and classified into different functional categories. To analyze the effect of the *cry1* mutation on each category, the percentage of up- and downregulated genes was calculated and compared. The RNA-seq data are available in the National Center for Biotechnology Information Sequence Read Archive under accession number SRP150048.

### SCW Thickness Analysis

The inflorescence stem at 0.5 cm above the rosette leaves was cut into 2-mm segments, which were fixed and used for observation of cell walls using a transmission electron microscope (Hitachi H-7650) according to previously published protocols (Zhao et al., 2014). SCW thickness was measured using ImageJ software. At least 30 cells were collected and analyzed statistically using a Student's *t* test.

### Analysis of SCW Chemical Components

Lignin and cellulose were determined as described with some modifications (Foster et al., 2010a, 2010b). Arabidopsis inflorescence stems were collected and ground to a fine powder in liquid nitrogen. Alcohol-insoluble residue (AIR) was obtained by successively washing the powder using 70% (v/v) ethanol, chloroform/methanol (1:1 v/v), and acetone. AIR was destarched using α-amylase (1 μg/mL) and pullulanase (10 units/mL) in 0.1 M sodium acetate buffer (pH 5.0), washed with water and acetone, and dried at 45°C for lignin and cellulose content determination.

#### *Lignin Content Determination*

Lignin Content Determination AIR (1–2 mg) was reacted with acetyl bromide solution (25% [v/v] acetyl bromide in glacial acetic acid), and the reaction was terminated with the addition of 2 M sodium hydroxide and 0.5 M hydroxylamine hydrochloride. The reaction mixture was then adjusted to a volume of 2 mL using glacial acetic acid and the absorbance was measured with Varioskan Flash 4.00.53 (Thermo Scientific) at $A_{280}$. The acetyl bromide soluble lignin content (% ABSL: percentage of the AIR [w/w]) was calculated according to a previously published method (Foster et al., 2010a, 2010b).

#### *Cellulose Content Determination*

Cellulose Content Determination AIR (1–2 mg) was incubated with 250 μL of 2 M trifluoroacetic acid for 90 min at 121°C and then centrifuged at 10,000 rpm for 10 min at room temperature after cooling on ice. The supernatant was removed and the pellet was thoroughly washed using water and acetone (repeated three times) and then dried in air. Sulfuric acid (72% [v/v]) was added to hydrolyze (room temperature, 1 h) the dried material into glucose, and its content was determined by colorimetric anthrone assay according to a previously published method (Foster et al., 2010a).

#### *Noncellulosic Polysaccharide Determination*

Noncellulosic Polysaccharide Determination AIR (1–2 mg) was washed with acetone, then hydrolyzed with 250 μL of 2 M trifluoroacetic acid for 90 min at 121°C. After cooled on ice and centrifuged at 10,000 rpm for 10 min at room temperature, 100 μL of the supernatant was applied to analyze noncellulosic polysaccharides. The supernatant was transferred to a new 2-mL screw cap tube and evaporated, then washed with 2-propanol. After evaporation. 200 μL of sodium borohydride solution (20 mg/mL in DMSO) was added to reduce the monosaccharides to their corresponding alditols at 40°C for 90 min. After reaction, 20 μL glacial acetic acid was added for neutralization. Then 25 μL of 1-methylimidazole and 250 μL acetic anhydride was added successively for acetylation at 120°C for 30 min. The reaction product was extracted with 1 mL of dichloromethane and washed by 1 mL of water three times. After evaporation, the product was dissolved in 200 μL of ethyl acetate and applied to GC-MS analysis (Agilent Technologies, 6890N GC system and 5975 mass detector; Supelco, SP-2380) according to a previously published method (Foster et al., 2010a).

### cDNA Library Construction of Arabidopsis Inflorescence Stem Tissue

Inflorescence stems were collected from 5-week-old Arabidopsis plants and used for mRNA isolation. Following the manufacturer's protocol, the inflorescence stem cDNA library was constructed in a pDEST22 vector using a Clone Miner II cDNA library construction kit from Invitrogen.

### Y1H Screening

The *NST1* promoter (3.7 kb) was subdivided into eight fragments (namely, *NST1P1*, *NST1P2*, *NST1P3*, *NST1P4*, *NST1P5*, *NST1P6*, *NST1P7*, and *NST1P8*), which were then cloned into a *pAbAi* vector. Then the constructs were transferred to yeast (Y1H-GOLD strain) to produce bait host cells and their self-activation activity was examined on the SD-Ura medium containing 100, 500, and 1000 ng/mL Aureobasidin A (AbA). Except for the *NST1P1*-containing cells, which showed self-activation in the Y1H system, the *NST1P2*∼*NST1P8* cells were used as the bait for further screening. For Y1H screening, the inflorescence stem cDNA library was transformed into the bait yeast cells and plated on the freshly prepared SD-Trp + 1 μg/mL AbA plates with >10,000 pfu/plate. Positive clones were collected through selection twice on SD-Trp + 1 μg/mL AbA plates and sequenced.

For confirmation, the coding sequence of collected clones was cloned into the *pDEST22* vector and transformed to bait yeast cells which contained the *NST1P6* fragment and tested on a SD-Trp + 500 ng/mL AbA plate.

### MYC2/MYC4 Transcriptional Activity Assay

MYC2/MYC4 transcriptional activity was examined using a dual-LUC reporter assay system (Promega) through protoplast transfection. The *MYC2* and *MYC4* coding sequences were cloned into *pA7* vector under the control of the *35S* promoter and used as an effector. The *NST1* (–1 to ∼–3711 from ATG) promoter sequence was cloned into the *pGreenII 0800-LUC* vector upstream of the *LUC* gene and used as a reporter. The *Renilla LUCIFERASE* (*REN*) gene in a *pGreenII0800-LUC* vector was used as an internal control. A VP16 transactivation domain sequence was amplified from *pBT3-N* and cloned into the *pA7* vector before the N-terminal/C-terminal or full length sequence of *MYC2*. All primers used in cloning are listed in Supplemental Table 2. Arabidopsis mesophyll protoplasts were prepared and transfected as described (Yoo et al., 2007). LUC activity was measured and normalized against the basal *Renilla* LUC activity in each transfection event.

### ChIP Assay

The *MYC2* and *MYC4* coding sequences were cloned into the *p1300-35S$_{pro}$-MYC2-3FLAG* and *p1300-35S$_{pro}$-MYC4-3HA* vectors and transferred into wild-type Arabidopsis and their encoded proteins were detected by immunoblot analysis (anti-FLAG/HA (catalog no. M20003L from Abmart). For ChIP analysis, inflorescence stems from three different transgenic lines of the T2 plants were analyzed. The immunoprecipitation analysis was performed according to a previously published method (Bowler et al., 2004) using a Magna ChIP A/G kit (Millipore). Total protein was extracted from the inflorescence stems of 4-week-old transgenic plants following Bowler's method. The bound DNA fragments were analyzed using RT-qPCR and *ACT2* was used as an internal control.

### Measurement of Tensile Strength

The tensile strength of the first internode of the inflorescence stem was measured using a HY0580 instrument (Shanghai Heng Yi Precision Instrument) with a 50 N sensor. Resultant force ("F") and stem diameter ("d") were measured and used to calculate tensile stress as follows: tensile stress, $\sigma = F/A$, $A = S = \pi^*(d/2)^2$

### Immunoblot Analysis

Immunoblot analysis was performed according to our previous study (Yu et al., 2013). Protein blots were first analyzed using either anti-FLAG/MYC (1:1000 dilution; Abmart) or anti-ACTIN2 (catalog no. M20009M) (1:2000 dilution; Abmart) monoclonal antibodies followed by goat-anti-mouse antibodies (1:5000 dilution, Thermo Fisher, catalog no. 31320). BCIP/ NBT (Life Technology) staining was used to visualize the blots.

### CRY1 Immunolocalization

Immunolocalization was performed according to the previous study (Song et al., 2010). Basal part ∼0.5 cm above the rosette leaves of the inflorescence stem from 5-week-old plants was fixed and embedded into paraffin and sectioned. The sections were blocked and then incubated with the CRY1 antibody or rabbit IgG (generated by Shanghai Youke Biotechnology) in blocking solution (1:200 dilution). After reacted with the secondary antibodies (1:5000 dilution, goat anti-rabbit antibody, Thermo Fisher Scientific, catalog no. 31,340), sections were stained with BCIP/NBT at room temperature and observed under a light microscope (Olympus BX51).

### Fiber Cell Analysis

Fiber cell length measurements, stem paraffin sections for fiber cell size measurement, and free-hand sections were conducted according to a previous study (Yu et al., 2013). For fiber cell length measurements, 2 cm of the bottom of the inflorescence stem segments was treated with glacial acetic acid and hydrogen peroxide (v/v 1:1), stained, and photographed under a light microscope (Olympus BX51). For fiber cell size measurements, the stem samples were fixed, embedded in paraffin, sectioned, stained with 0.05% toluidine blue, and photographed for analysis. The fiber cell length and fiber cell size were measured using ImageJ software.

### Promoter GUS Activity Analysis

*MYC2* promoter (–1 to ∼–3226 from ATG) and *MYC4* promoter (–1 to ∼–1633 from ATG) were cloned into a *p1301* vector to drive the *GUS* expression. After wild-type Arabidopsis was transformed with the promoter constructs, the T2 transgenic plants were used to analyze the GUS staining activity. GUS staining was performed according to a previous study (Yu et al., 2013).

### Accession Numbers

Sequence data from this article can be found at https://www.arabidopsis.org with the following accession numbers: *CRY1* (AT4G08920), *MYC2* (AT1G32640), *MYC3* (AT5G46760), *MYC4* (AT4G17880), *MYC5* (At5G46830), *SND1* (AT1G32770), *NST1* (AT2G46770), *CESA4* (AT5G44030), *IRX8* (AT5G54690), *4CL1* (AT1G51680), and *ACT2* (AT3G18780).

### Supplemental Data

**Supplemental Figure 1.** *CRY1* affects elongation growth and SCW thickening in the inflorescence stem.

**Supplemental Figure 2.** The red light-treated *cry1* mutant shows minor differences in SCW thickening in the fiber cells of inflorescence stem compared with the wild type.

**Supplemental Figure 3.** Tensile strength at the basal region of the inflorescence stem in *NST1-OE* and *snd1 nst1* plants.

**Supplemental Figure 4.** Sugar composition of the noncellulosic polysaccharides in the inflorescence stem of wild-type, *cry1*, and *CRY1-OE* plants grown in blue light.

**Supplemental Figure 5.** *CRY1* expression correlates with SCW thickening.

**Supplemental Figure 6.** Expression patterns of the candidate genes identified by yeast one-hybrid assay.

**Supplemental Figure 7.** Detection of MYC2 binding and activation to the *NST1* promoter.

**Supplemental Figure 8.** *MYC2* genetically interacted with *CRY1*.

**Supplemental Figure 9.** Promoter activity of *MYC2* and *MYC4*.

**Supplemental Figure 10.** Sugar composition of noncellulosic polysaccharides in *myc2 myc4* inflorescence stems grown in blue light.

**Supplemental Figure 11.** *MYC2* overexpression led to an increase in the expression of the SCW formation related genes.

**Supplemental Data Set 1.** Summary of transcriptome analysis of the inflorescence stem of *cry1* mutants.

**Supplemental Table 1.** Candidate genes identified by yeast one-hybrid assays.

**Supplemental Table 2.** Primer sequences used in this study.

## ACKNOWLEDGMENTS

We thank Daoxin Xie (Tsinghua University) for providing *myc2 myc4* mutants. We thank Jiechen Wang for providing *pAbAi* vectors and *Y1H-Gold* strains; Xiaoyan Gao, Zhiping Zhang, Jiqin Li, Fenglin Qin, and Xu Wang for assistance with transmission electron microscopy; and Wenli Hu for assistance with GC-MS analysis. This work was supported by the National Nature Science Foundation of China (31630014), the Ministry of Science and Technology of China (2016YFD0600104), and the Chinese Academy of Sciences (XDPB0402).

## AUTHOR CONTRIBUTIONS

Q.Z., H.L., H.Y., and L.L. designed the research. Q.Z., Z.X., and R.Z. performed the experiments. Q.Z., P.X., H.L., H.Y., M.S.D., A.B., and L.L. analyzed the data. Q.Z, M.S.D., A.B., and L.L. wrote the article. All authors read and approved the article.

Received April 19, 2018; revised September 5, 2018; accepted September 16, 2018; published September 21, 2018.

## REFERENCES

**Ahmad, M., and Cashmore, A.R.** (1993). HY4 gene of *A. thaliana* encodes a protein with characteristics of a blue-light photoreceptor. Nature **366:** 162–166.

**Bischoff, V., Desprez, T., Mouille, G., Vernhettes, S., Gonneau, M., and Höfte, H.** (2011). Phytochrome regulation of cellulose synthesis in Arabidopsis. Curr. Biol. **21:** 1822–1827.

**Bowler, C., Benvenuto, G., Laflamme, P., Molino, D., Probst, A.V., Tariq, M., and Paszkowski, J.** (2004). Chromatin techniques for plant cells. Plant J. **39:** 776–789.

**Boyle, E.I., Weng, S., Gollub, J., Jin, H., Botstein, D., Cherry, J.M., and Sherlock, G.** (2004). GO:TermFinder--open source software for accessing Gene Ontology information and finding significantly enriched Gene Ontology terms associated with a list of genes. Bioinformatics **20:** 3710–3715.

**Caño-Delgado, A., Lee, J.-Y., and Demura, T.** (2010). Regulatory mechanisms for specification and patterning of plant vascular tissues. Annu. Rev. Cell Dev. Biol. **26:** 605–637.

**Chen, Q., et al.** (2011). The basic helix-loop-helix transcription factor MYC2 directly represses PLETHORA expression during jasmonate-mediated modulation of the root stem cell niche in Arabidopsis. Plant Cell **23:** 3335–3352.

**Chen, R., Jiang, H., Li, L., Zhai, Q., Qi, L., Zhou, W., Liu, X., Li, H., Zheng, W., Sun, J., and Li, C.** (2012). The Arabidopsis mediator subunit MED25 differentially regulates jasmonate and abscisic acid signaling through interacting with the MYC2 and ABI5 transcription factors. Plant Cell **24:** 2898–2916.

**Clough, S.J., and Bent, A.F.** (1998). Floral dip: a simplified method for Agrobacterium-mediated transformation of *Arabidopsis thaliana*. Plant J. **16:** 735–743.

**Dombrecht, B., Xue, G.P., Sprague, S.J., Kirkegaard, J.A., Ross, J.J., Reid, J.B., Fitt, G.P., Sewelam, N., Schenk, P.M., Manners, J.M., and Kazan, K.** (2007). MYC2 differentially modulates diverse jasmonate-dependent functions in Arabidopsis. Plant Cell **19:** 2225–2245.

**Fernández-Calvo, P., et al.** (2011). The Arabidopsis bHLH transcription factors MYC3 and MYC4 are targets of JAZ repressors and act additively with MYC2 in the activation of jasmonate responses. Plant Cell **23:** 701–715.

**Figueroa, P., and Browse, J.** (2015). Male sterility in Arabidopsis induced by overexpression of a MYC5-SRDX chimeric repressor. Plant J. **81:** 849–860.

**Foster, C.E., Martin, T.M., and Pauly, M.** (2010a). Comprehensive compositional analysis of plant cell walls (lignocellulosic biomass) part II: carbohydrates. J. Vis. Exp. **pii:** 1837.

**Foster, C.E., Martin, T.M., and Pauly, M.** (2010b). Comprehensive compositional analysis of plant cell walls (lignocellulosic biomass) part I: lignin. J. Vis. Exp. **pii:** 1745.

**Gangappa, S.N., Prasad, V.B., and Chattopadhyay, S.** (2010). Functional interconnection of MYC2 and SPA1 in the photomorphogenic seedling development of Arabidopsis. Plant Physiol. **154:** 1210–1219.

**Gao, C., Qi, S., Liu, K., Li, D., Jin, C., Li, Z., Huang, G., Hai, J., Zhang, M., and Chen, M.** (2016). MYC2, MYC3, and MYC4 function redundantly in seed storage protein accumulation in Arabidopsis. Plant Physiol. Biochem. **108:** 63–70.

**Gasperini, D., Chételat, A., Acosta, I.F., Goossens, J., Pauwels, L., Goossens, A., Dreos, R., Alfonso, E., and Farmer, E.E.** (2015). Multilayered organization of jasmonate signalling in the regulation of root growth. PLoS Genet. **11:** e1005300.

**Hao, Z., et al.** (2014). Loss of Arabidopsis GAUT12/IRX8 causes anther indehiscence and leads to reduced G lignin associated with altered matrix polysaccharide deposition. Front. Plant Sci. **5:** 357.

**Hectors, K., Jacques, E., Prinsen, E., Guisez, Y., Verbelen, J.P., Jansen, M.A., and Vissenberg, K.** (2010). UV radiation reduces epidermal cell expansion in leaves of *Arabidopsis thaliana*. J. Exp. Bot. **61:** 4339–4349.

**Hong, G.J., Xue, X.Y., Mao, Y.B., Wang, L.J., and Chen, X.Y.** (2012). Arabidopsis MYC2 interacts with DELLA proteins in regulating sesquiterpene synthase gene expression. Plant Cell **24:** 2635–2648.

**Hoson, T., and Wakabayashi, K.** (2015). Role of the plant cell wall in gravity resistance. Phytochemistry **112:** 84–90.

**Huber, H., de Brouwer, J., von Wettberg, E.J., During, H.J., and Anten, N.P.** (2014). More cells, bigger cells or simply reorganization? Alternative mechanisms leading to changed internode architecture under contrasting stress regimes. New Phytol. **201:** 193–204.

**Hussey, S.G., Mizrachi, E., Creux, N.M., and Myburg, A.A.** (2013). Navigating the transcriptional roadmap regulating plant secondary cell wall deposition. Front. Plant Sci. **4:** 325.

**Kazan, K., and Manners, J.M.** (2013). MYC2: the master in action. Mol. Plant **6:** 686–703.

**Keller, M.M., Jaillais, Y., Pedmale, U.V., Moreno, J.E., Chory, J., and Ballaré, C.L.** (2011). Cryptochrome 1 and phytochrome B control shade-avoidance responses in Arabidopsis via partially independent hormonal cascades. Plant J. **67:** 195–207.

**Keuskamp, D.H., Sasidharan, R., Vos, I., Peeters, A.J., Voesenek, L.A., and Pierik, R.** (2011). Blue-light-mediated shade avoidance requires combined auxin and brassinosteroid action in Arabidopsis seedlings. Plant J. **67:** 208–217.

**Kim, D., Langmead, B., and Salzberg, S.L.** (2015). HISAT: a fast spliced aligner with low memory requirements. Nat. Methods **12:** 357–360.

**Kim, J., Song, K., Park, E., Kim, K., Bae, G., and Choi, G.** (2016). Epidermal phytochrome B inhibits hypocotyl negative gravitropism non-cell-autonomously. Plant Cell **28:** 2770–2785.

**Koning, R.E.** (1994). Blue-light responses. In Plant Physiology Information Website, http://plantphys.info/plant_physiology/bluelight.shtml.

**Kumar, M., Campbell, L., and Turner, S.** (2016). Secondary cell walls: biosynthesis and manipulation. J. Exp. Bot. **67:** 515–531.

**Langmead, B., Trapnell, C., Pop, M., and Salzberg, S.L.** (2009). Ultrafast and memory-efficient alignment of short DNA sequences to the human genome. Genome Biol. **10:** R25.

**Lee, H.-J., et al.** (2016). Stem-piped light activates phytochrome B to trigger light responses in *Arabidopsis thaliana* roots. Sci. Signal. **9:** ra106.

**Lee, D., Meyer, K., Chapple, C., and Douglas, C.J.** (1997). Antisense suppression of 4-coumarate:coenzyme A ligase activity in Arabidopsis leads to altered lignin subunit composition. Plant Cell **9:** 1985–1998.

**Le Gall, H., Philippe, F., Domon, J.-M., Gillet, F., Pelloux, J., and Rayon, C.** (2015). Cell wall metabolism in response to abiotic stress. Plants (Basel) **4:** 112–166.

**Li, B., and Dewey, C.N.** (2011). RSEM: accurate transcript quantification from RNA-Seq data with or without a reference genome. BMC Bioinformatics **12:** 323.

**Li, X., Wang, Q., Yu, X., Liu, H., Yang, H., Zhao, C., Liu, X., Tan, C., Klejnot, J., Zhong, D., and Lin, C.** (2011). Arabidopsis cryptochrome 2 (CRY2) functions by the photoactivation mechanism distinct from the tryptophan (trp) triad-dependent photoreduction. Proc. Natl. Acad. Sci. USA **108:** 20844–20849.

**Lin, C.** (2000a). Plant blue-light receptors. Trends Plant Sci. **5:** 337–342.

**Lin, C.** (2000b). Photoreceptors and regulation of flowering time. Plant Physiol. **123:** 39–50.

**Lin, C., Yang, H., Guo, H., Mockler, T., Chen, J., and Cashmore, A.R.** (1998). Enhancement of blue-light sensitivity of Arabidopsis seedlings by a blue light receptor cryptochrome 2. Proc. Natl. Acad. Sci. USA **95:** 2686–2690.

**Liu, H., Yu, X., Li, K., Klejnot, J., Yang, H., Lisiero, D., and Lin, C.** (2008). Photoexcited CRY2 interacts with CIB1 to regulate transcription and floral initiation in Arabidopsis. Science **322:** 1535–1539.

**Liu, H., Liu, B., Zhao, C., Pepper, M., and Lin, C.** (2011). The action mechanisms of plant cryptochromes. Trends Plant Sci. **16:** 684–691.

**Lucas, W.J., et al.** (2013). The plant vascular system: evolution, development and functions. J. Integr. Plant Biol. **55:** 294–388.

**Maurya, J.P., Sethi, V., Gangappa, S.N., Gupta, N., and Chattopadhyay, S.** (2015). Interaction of MYC2 and GBF1 results in functional antagonism in blue light-mediated Arabidopsis seedling development. Plant J. **83:** 439–450.

**Mitsuda, N., Seki, M., Shinozaki, K., and Ohme-Takagi, M.** (2005). The NAC transcription factors NST1 and NST2 of Arabidopsis regulate secondary wall thickenings and are required for anther dehiscence. Plant Cell **17:** 2993–3006.

**Mitsuda, N., Iwase, A., Yamamoto, H., Yoshida, M., Seki, M., Shinozaki, K., and Ohme-Takagi, M.** (2007). NAC transcription factors, NST1 and NST3, are key regulators of the formation of secondary walls in woody tissues of Arabidopsis. Plant Cell **19:** 270–280.

**Mortazavi, A., Williams, B.A., McCue, K., Schaeffer, L., and Wold, B.** (2008). Mapping and quantifying mammalian transcriptomes by RNA-seq. Nat. Methods **5:** 621–628.

**Phee, B.K., Park, S., Cho, J.H., Jeon, J.S., Bhoo, S.H., and Hahn, T.R.** (2007). Comparative proteomic analysis of blue light signaling components in the Arabidopsis cryptochrome 1 mutant. Mol. Cells **23:** 154–160.

**Qi, T., Huang, H., Song, S., and Xie, D.** (2015). Regulation of jasmonate-mediated stamen development and seed production by a bHLH-MYB complex in Arabidopsis. Plant Cell **27:** 1620–1633.

**Reed, J.W., Nagpal, P., Poole, D.S., Furuya, M., and Chory, J.** (1993). Mutations in the gene for the red/far-red light receptor phytochrome B alter cell elongation and physiological responses throughout Arabidopsis development. Plant Cell **5:** 147–157.

**Robson, T.M., Klem, K., Urban, O., and Jansen, M.A.** (2015). Re-interpreting plant morphological responses to UV-B radiation. Plant Cell Environ. **38:** 856–866.

**Ruonala, R., Ko, D., and Helariutta, Y.** (2017). Genetic networks in plant vascular development. Annu. Rev. Genet. **51:** 335–359.

**Sang, Y., Li, Q.H., Rubio, V., Zhang, Y.C., Mao, J., Deng, X.W., and Yang, H.Q.** (2005). N-terminal domain-mediated homodimerization is required for photoreceptor activity of Arabidopsis CRYPTOCHROME 1. Plant Cell **17:** 1569–1584.

**Sasidharan, R., Chinnappa, C.C., Staal, M., Elzenga, J.T.M., Yokoyama, R., Nishitani, K., Voesenek, L.A.C.J., and Pierik, R.** (2010). Light quality-mediated petiole elongation in Arabidopsis during shade avoidance involves cell wall modification by xyloglucan endotransglucosylase/hydrolases. Plant Physiol. **154:** 978–990.

**Schuetz, M., Smith, R., and Ellis, B.** (2013). Xylem tissue specification, patterning, and differentiation mechanisms. J. Exp. Bot. **64:** 11–31.

**Sellaro, R., Crepy, M., Trupkin, S.A., Karayekov, E., Buchovsky, A.S., Rossi, C., and Casal, J.J.** (2010). Cryptochrome as a sensor of the blue/green ratio of natural radiation in Arabidopsis. Plant Physiol. **154:** 401–409.

**Sethi, V., Raghuram, B., Sinha, A.K., and Chattopadhyay, S.** (2014). A mitogen-activated protein kinase cascade module, MKK3-MPK6 and MYC2, is involved in blue light-mediated seedling development in Arabidopsis. Plant Cell **26:** 3343–3357.

**Song, D., Shen, J., and Li, L.** (2010). Characterization of cellulose synthase complexes in Populus xylem differentiation. New Phytol. **187:** 777–790.

**Song, S., Huang, H., Gao, H., Wang, J., Wu, D., Liu, X., Yang, S., Zhai, Q., Li, C., Qi, T., and Xie, D.** (2014). Interaction between MYC2 and ETHYLENE INSENSITIVE3 modulates antagonism between jasmonate and ethylene signaling in Arabidopsis. Plant Cell **26:** 263–279.

**Tarazona, S., García-Alcalde, F., Dopazo, J., Ferrer, A., and Conesa, A.** (2011). Differential expression in RNA-seq: a matter of depth. Genome Res. **21:** 2213–2223.

**Taylor, N.G., Howells, R.M., Huttly, A.K., Vickers, K., and Turner, S.R.** (2003). Interactions among three distinct CesA proteins essential for cellulose synthesis. Proc. Natl. Acad. Sci. USA **100:** 1450–1455.

**Taylor-Teeples, M., et al.** (2015). An Arabidopsis gene regulatory network for secondary cell wall synthesis. Nature **517:** 571–575.

**Underwood, W.** (2012). The plant cell wall: a dynamic barrier against pathogen invasion. Front. Plant Sci. **3:** 85.

**Wang, Z., Gerstein, M., and Snyder, M.** (2009). RNA-Seq: a revolutionary tool for transcriptomics. Nat. Rev. Genet. **10:** 57–63.

**Wargent, J.J., Moore, J.P., Roland Ennos, A., and Paul, N.D.** (2009). Ultraviolet radiation as a limiting factor in leaf expansion and development. Photochem. Photobiol. **85:** 279–286.

**Wu, L., Zhang, W., Ding, Y., Zhang, J., Cambula, E.D., Weng, F., Liu, Z., Ding, C., Tang, S., Chen, L., Wang, S., and Li, G.** (2017). Shading contributes to the reduction of stem mechanical strength by decreasing cell wall synthesis in japonica rice (*Oryza sativa* L.). Front. Plant Sci. **8:** 881.

**Yadav, V., Mallappa, C., Gangappa, S.N., Bhatia, S., and Chattopadhyay, S.** (2005). A basic helix-loop-helix transcription factor in Arabidopsis, MYC2, acts as a repressor of blue light-mediated photomorphogenic growth. Plant Cell **17:** 1953–1966.

**Yamaguchi, M., Kubo, M., Fukuda, H., and Demura, T.** (2008). Vascular-related NAC-DOMAIN7 is involved in the differentiation of all types of xylem vessels in Arabidopsis roots and shoots. Plant J. **55:** 652–664.

**Yamaguchi, M., Goué, N., Igarashi, H., Ohtani, M., Nakano, Y., Mortimer, J.C., Nishikubo, N., Kubo, M., Katayama, Y., Kakegawa, K., Dupree, P., and Demura, T.** (2010). VASCULAR-RELATED NAC-DOMAIN6 and VASCULAR-RELATED NAC-DOMAIN7 effectively induce transdifferentiation into xylem vessel elements under control of an induction system. Plant Physiol. **153:** 906–914.

**Yamaguchi, M., Mitsuda, N., Ohtani, M., Ohme-Takagi, M., Kato, K., and Demura, T.** (2011). VASCULAR-RELATED NAC-DOMAIN7 directly regulates the expression of a broad range of genes for xylem vessel formation. Plant J. **66:** 579–590.

**Yoo, S.D., Cho, Y.H., and Sheen, J.** (2007). Arabidopsis mesophyll protoplasts: a versatile cell system for transient gene expression analysis. Nat. Protoc. **2:** 1565–1572.

**Yu, L., Sun, J., and Li, L.** (2013). PtrCel9A6, an endo-1,4-β-glucanase, is required for cell wall formation during xylem differentiation in populus. Mol. Plant **6:** 1904–1917.

**Zhang, X., Zhu, Z., An, F., Hao, D., Li, P., Song, J., Yi, C., and Guo, H.** (2014). Jasmonate-activated MYC2 represses ETHYLENE INSENSITIVE3 activity to antagonize ethylene-promoted apical hook formation in Arabidopsis. Plant Cell **26:** 1105–1117.

**Zhao, Y., Sun, J., Xu, P., Zhang, R., and Li, L.** (2014). Intron-mediated alternative splicing of WOOD-ASSOCIATED NAC TRANSCRIPTION FACTOR1B regulates cell wall thickening during fiber development in Populus species. Plant Physiol. **164:** 765–776.

**Zhong, R., and Ye, Z.H.** (2014). Complexity of the transcriptional network controlling secondary wall biosynthesis. Plant Sci. **229:** 193–207.

**Zhong, R., and Ye, Z.H.** (2015). Secondary cell walls: biosynthesis, patterned deposition and transcriptional regulation. Plant Cell Physiol. **56:** 195–214.

**Zhong, R., Demura, T., and Ye, Z.H.** (2006). SND1, a NAC domain transcription factor, is a key regulator of secondary wall synthesis in fibers of Arabidopsis. Plant Cell **18:** 3158–3170.

**Zhong, R., Richardson, E.A., and Ye, Z.H.** (2007). Two NAC domain transcription factors, SND1 and NST1, function redundantly in regulation of secondary wall synthesis in fibers of Arabidopsis. Planta **225:** 1603–1611.

**Zhong, R., Lee, C., Zhou, J., McCarthy, R.L., and Ye, Z.H.** (2008). A battery of transcription factors involved in the regulation of secondary cell wall biosynthesis in Arabidopsis. Plant Cell **20:** 2763–2782.

**Zhong, R., Lee, C., and Ye, Z.H.** (2010). Global analysis of direct targets of secondary wall NAC master switches in Arabidopsis. Mol. Plant **3:** 1087–1103.